Long Term Effect of Climate Change on Rainfall in Northwest Iraq

Abstract

Middle East and North Africa are considered as arid to semi-arid region. Water shortages in this region, represents an extremely important factor in the stability of the region and an integral element in its economic development and prosperity. Iraq was an exception due to the presence of Tigris and Euphrates Rivers. After the 1970s the situation began to deteriorate due to continuous decrease of the discharges of these rivers which are expected to dry (2040) with global climate change. In this research, long rainfall trends up to the year 2099 were studied in Sinjar area, northwest of Iraq to give an idea about future prospects. Two emission scenarios used by the Intergovernmental Panel on Climate Change (A2 & B2) were employed to study long term rainfall trends in northwest of Iraq. ANN model was used to provide climate change information at a suitable spatial scale from the Global Climate Model (GCM) data. In general 7 predictors of climate variables were found to have a significant relation with the rainfall for winter, spring and 6 predictors for autumn while the summer shows only 4 predictors. All seasons consistently projected a drop in daily rainfall for all future periods with summer which expected to have more reduction compared with other seasons as it is consider to be almost dry by end of 21 century for both scenarios. The results also indicates that, there is an appreciable change in the number of wet days by 2080s for months January, February and March in both scenarios with about 10%-40% decrease in wet days, while rest of the months experience a slight drop for all future periods. Summer months are noticed are considered almost dry, however, a tendency of dryness extending to September is also observed. Generally the average rainfall trend shows a continuous decrease. The overall average annual rainfall is slightly above 210 mm. In view of this prudent water management strategies are to be adopted to overcome water shortage crisis.

Key words: Rainfall trend, GCM, ANN, Sinjar, Iraq

1.0 Introduction

Middle East and North Africa (MENA region) are considered as arid to semi-arid regions where the average annual rainfall does not exceed 166mm (Al-Ansari, 1998). For this reason, the scarcity of water resources in the MENA region, and particularly in the Middle East, represents an extremely important factor in the stability of the region and an integral element in its economic development and prosperity (Naff, 1993 and Al-Ansari, 2005). Recent work indicates that the situation will be more severe in future (Bazzaz, 1993 and Voss, et.al, 2013). Climate change is one of the main factors for future shortages expected in the region (Al-Ansari, 2013). At the end of this century the mean temperatures in the MENA region are projected to increase by 3°C to 5°C while the precipitation will decrease by about 20% (Elasha, 2010). Water run-off will be reduced by 20% to 30% in most of MENA by 2050 (IP CC, 2007) and water supply might be reduced by 10% or greater by 2050 (Milly et. al., 2005).

Iraq till the 1970s was considered rich in its water resources due to the presence of the Tigris and Euphrates Rivers. Syria and Turkey started to build dams on the upper parts of these rivers which caused a major decrease in the flow of the rivers (Al-Ansari and Knutsson, 2011). Tigris and Euphrates discharges will continue to decrease with time and they will be completely dry up by 2040(UN, 2010). In addition, future rainfall forecast showed that it is decreasing in Jordan which is Iraq's neighboring country (Al-Ansari, et.al, 1999&2006, Al-Ansari and Baban, 2005).

In this paper, statistical downscaling models which were constructed with ANN of ALevenberg-Marquardt approach were used to evaluate long term rainfall amounts expected in northwest Iraq for

four seasons (winter, spring, summer and autumn). This will help farmers and decision makers to take precautions to overcome water shortages.

2.0 Studied Region & Data

Sinjar District is a plan area located within Nineveh province in northwest Iraq (Figure 1). The whole area is locally referred to as Al-Jazirah (the area bounded by the Tigris and Euphrates Rivers north of Tharthar Lake). It is bordered from north and west by the international Iraq-Syria borders and the extension Province of Nineveh from the east and south. The population reaches 21,584. The most prominent terrain is Sinjar Mountain with highest peak that reaches an elevation of 1400 (m. a. s. l.) (Figure 1). Rain water is the main source for agricultural practices in Sinjar area despite the presence of some wells.

The average annual rainfall records indicate that it is about 303 mm. The rainy season extends from November to May. During this season, surface water flows in the valleys from Sinjar Mountain toward the Iraqi-Syrian border at northern Sinjar Mountain, and flows to the extension Province of Nineveh at southern Sinjar Mountain. Maximum monthly evaporation is usually recorded in July and reaches 563.4 mm. The value drops to 57.4 mm in December. The soil in the study area has low organic content and consists of sandy loam, silty loam and silty clay loam (Rasheed, et.al., 1994). Fields observation indicates that, the catchment area at Sinjar region is one of three types: cultivated land, pasture land, and land covered by exposures of hard rocks. The cultivated land represents very good farming conditions (Figure 2) and has the ability to produce main crops such as wheat, barley and tobacco if water is available.

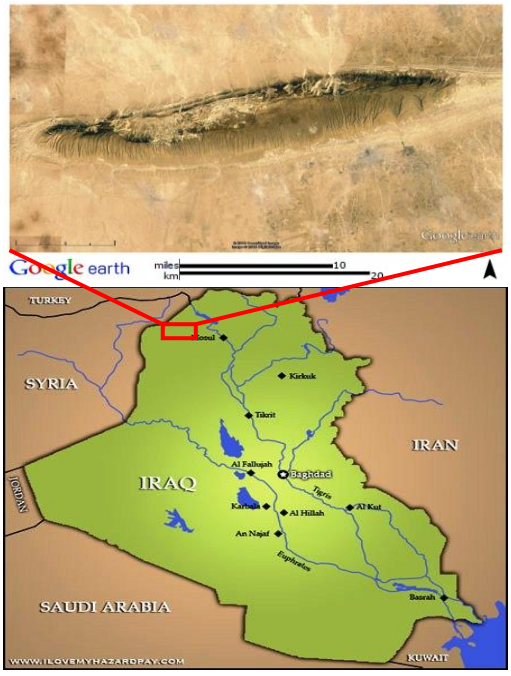

Figure 1 Sinjar area

Figure 2 Farm at Sinjar area.

Suitable data are needed to understand and investigate the relationship between hydrology and climate change. Two principal data sets were employed during the calibration, validation and simulation of the daily rainfall models:

First, Rainfall data which is one of the main components in the hydrological cycle and intimately linked with almost all aspect of climate. Therefore rainfall data of highest quality are of primary importance for hydrological calculations. The main rainfall data used here are daily observations obtained from Iraqi Meteorological Office for period 1961-2001.

Second, atmospheric data, these variables were used for the purpose of constructing a rainfall model (observed) and to simulate the future climate from GCM. Both observed and GCM daily predictor variables have been normalised with respect to their 1961-1990 means and standard deviations to account for any bias from the GCM. The normalisation process ensures that the distributions of observed and GCM-derived predictors are in closer agreement than those of the raw observed and raw GCM data. These two sets (large scale predictors) are described below:

A. Reanalysis data

Reanalysis data provide baselines or climate reference for future climate projections. The US National Centres for Environmental Prediction (NCEP) reanalysis dataset (Kalnay et al. 1996) provides contemporaneous gridded data which is usually considered to be the best global climate circulation representation of the current state of the earth system. NCEP data originally at resolution of 2.5^0x2.5^0, was re-gridded to conform to output of the GCM and was selected at grid box covering each of the station. The NCEP data are however considered adequate for present purposes, i.e. to be used as the current observed atmospheric data for developing downscaling rainfall (calibration and validation) tools using global climate data and was obtained for the period 1961-2001.

B. Climate Model Data

With provision for the simulation of the effects of anthropogenic emissions, climate models are an important tool for providing future climate information (Wheater, 2002). HadCM3 Global Climate Model (GCM) with grid resolution of 2.5^0x3.75^0 is used in this paper to provide future climate scenarios for three future periods 2020s (2010-2039), 2050s (2040-2069) and 2080s (2070-2099). Since climate projections are related to emission uncertainty, different climate scenarios, defined by Nakicenovic et al. (2000), are used by the Intergovernmental Panel on Climate Change to account for the uncertainty of future anthropogenic carbon emissions. Both the A2 & B2 emission scenarios are employed here.

2.0 Methodology

GCMs are the main tools to predict large scale climate variations at seasonal and interannual scales, but they are usually not successful in reproducing higher order statistics and extreme values. Furthermore, they can not be adapted for impact-oriented applications at regional scale because of their relatively coarse resolution of typically several hundred kilometers (Von and Heckl, 2011). For bridging the gap

between the scale of GCM and required resolution for practical applications, downscaling provides climate change information at a suitable spatial scale from the GCM data.

In this study a downscaling approach has been used to obtain local scale rainfall at Sinjar station employing two steps, selected the suitable clime variables (predictors) and then developing the rainfall model.

2.1 Model Predictors

For downscaling rainfall, the selection of appropriate predictors is one of the most important steps in a downscaling exercise. The predictors are chosen by the following criteria: (1) they should be skillful in representing large-scale variability that is simulated by the GCMs and are readily available from archives of GCM output and reanalysis data sets; (2) they should strongly correlated with the with the surface variables of interest/predictands i.e. they should be statistically significant contributors to the variability in rainfall; (3) they should represent important physical processes in the context of the enhanced greenhouse effect (Hewitson and Crane, 1996; Cavazos and Hewitson, 2005). The stepwise regression has been used for purpose of this process in order to select the parsimonious model as it would generally not be useful to include all predictors in the final model. The stepwise selection procedure is the combination of forward selection and backward elimination after adding one predictor to the subset or excluding one predictor from the subset. In this process, the observed daily predictors (climatic variables), which come from NCEP data, are selected from a range of candidate predictors that correlated with daily rainfall data for each season winter(JFD), spring(MAM), summer(JJA) and autumn(SON).

2.2 Rainfall Model

The daily single-site rainfall downscaling model is used in this study is ANN which has been recently used in many single or multisite daily rainfall generation as well as downscaling applications (for example, Ojha et al., 2010; Hoai et al., 2011; Fistikoglu and Okkan, 2011). ANNs is an example of the regression statistical downscaling method and has potential for complex, nonlinear, and time varying input-output mapping and rely on empirical relationships between local-scale predictands and regional-scale predictor(s). Although the weights of an ANN are similar to nonlinear regression coefficients, the unique structure of the network and the nonlinear transfer function associated with each hidden and output node allows ANNs to approximate highly nonlinear relationships. Therefore the interest in ANNs is nowadays increasing (Coulibaly and Dibike, 2004).

The model simulates rainfall wet and dry day at each location and is formulated to reproduce the temporal structure of the observed rainfall record in the simulations. On a given day, the model simulates rainfall at Sinjar station conditional on selected atmospheric variables for each season.

2.2.1 ANN Model Structure

The multi-layer feed forward ANN (MLF-ANN) (see Figure 3) composed of multiple simple processing nodes, or neurons, assembled in different layers (input, hidden, output). Each node computes a linear combination of the weighted inputs including a bias term from the links feeding into it. The assumed value of these inputs is transformed using a certain activation function; either linear or non-linear. The output obtained is then passed as input to other nodes in the following layer. One important requirement for this activation function is that it must map any input to a finite output range, usually between 0 and 1 or -1 and 1 (Lisboa, 1992). Several different activation functions can be used, in this study, the linear (output layer) and log-sigmoid (hidden layer) have been selected which are commonly used. Figure 1 show a typical three layer MLF, the output 'y' (rainfall) of a network with 'n' inputs, '*k*' log-sigmoid nodes in the hidden layer and one linear node in the output layer is given by:

$$y = \sum_1^k w_j^{(2)} \; z_j + \; b^{(2)} \tag{1}$$

$$Z_j = f\left(\sum_1^m w_{ij}^{(1)} \; X_i \quad + b_j^{(1)}\right) = \frac{1}{1+\exp\left(\sum_1^m -w_{ij}^{(1)} x_i + b_j^{(1)}\right)} \tag{2}$$

where,

X_i corresponds to the ith input (selected climatic variables)

$w_j^{(2)}$ and $b^{(2)}$ ($w_{ij}^{(1)}$ and $b_j^{(1)}$) are the weights and biases from the output (hidden) layers

f is the log-sigmoid transfer function.

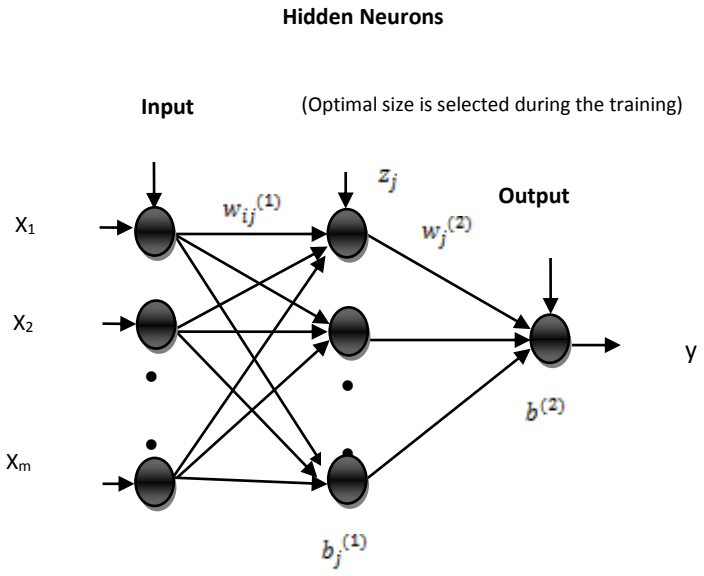

Figure 3 Multilayer feed forward ANN

2.2.2 Training of MLF-ANN

The training of ANN simply means estimation of the model parameters which are the weights and number of hidden neurons. The main objective behind all ANN training algorithm is to minimise a certain error function *E*. The quantity *E*, usually the Mean Square Error, measures the difference between the observed (*O*) and predicted (*S*) values for a data with size (n) (Trigo 2000),

$$E = \frac{1}{n}\left(\sum_i^n \left(O(i) - S(i)\right)^2\right) \quad (3)$$

For MLF-ANN, with more than one layer of weights (as in Figure 1), the error function will typically be a highly non-linear function of weights. As consequences of non-linearity, it is not in general possible to find an analytical solution for the minimum of the *E*. Instead, it is necessary to consider algorithm that involves a search through the weight space consisting of a succession of steps.

Different algorithms involve different techniques to define the weight .The training technique most widely used in literature is the backpropagation algorithm in which the error is then back propagated through the network and weights are adjusted as the network attempts to decrease the prediction error by optimising the weights that contribute most to the error. This process is repeated many times with many different hidden neurons pairs until a sufficient accuracy for all data sets has been obtained. There are different backpropagation algorithms, however in the present application, Levenberg-Marquardt approach (LM) has been applied and that distinguish the current paper from the conventional ANN algorithm used.

The LM algorithm which was independently developed by Kenneth Levenberg and Donald Marquardt (Levenberg, 1944; Marquardt, 1963) provides a numerical solution to the problem of minimizing a nonlinear function. It is usually more stable and more reliable than any other back-propagation techniques, and was designed to speed up the training process (Jeong and Kim, 2005; Yadav et al., 2010). LM is based on the approximation of Gauss-Newton method and introduces another approximation to the Hessian matrix, H defined as:

$$H = J^T J + \mu I \quad (4)$$

μ is always positive, called combination coefficient

I is the identity matrix

J is the Jacobian matrix and can be computed through a standard backpropagation technique that is much less complex than computing the Hessian matrix. The Jacobian contains the first derivatives of the ANN errors with respect to weights. So the update rule of LM algorithm can be presented as;

$$w_{k+1} = w_k - (J^T J + \mu I)^{-1} J^T e \quad (5)$$

2.2.3 Model Evaluation techniques

Part of daily rainfall within the period 1961-2001 was used for verification processes for each of the winter, spring, summer and autumn models. The performances of the ANN model were evaluated mainly based on:

1. The correlation coefficient (*R*) has been widely used to evaluate the goodness-of-fit of hydrologic and hydrodynamic models (Legates and McCabe, 1999). This is obtained by performing a linear

regression between the ANN-predicted values (*S*) and the targets for n observations (*O*), being defined as,

$$R = \frac{\sum_{i}^{n}(O-\bar{S})(S-\bar{S})}{\left(\sum_{i}^{n}\left(S-\bar{S}\right)^{2}\sum_{i}^{n}\left(S-\bar{S}\right)^{2}\right)^{1/2}} \tag{6}$$

A case with *R* is equal to 1 refers to a perfect correlation and the predicted values are either equal or very close to the target values, whereas there exists a case with no correlation between the predicted and the target values when *R* is equal to zero. Intermediate values closer to 1 indicate better agreement between target and predicted values (Legates and McCabe, 1999).

2. Root Mean Squared Error (*RMSE*) for n observations (Schaap and Leij, 1998) defined as,

$$RMSE = \sqrt{\frac{\sum_{i=1}^{n}\left(O_i - S_i\right)^2}{n}} \tag{7}$$

ANN responses are more precise if RMSE close to (0).

3. Nash –Sutcliffe coefficient. The range of this coefficient lies between 1.0 (perfect fit) and$-\infty$. An efficiency of lower than zero indicates that the mean value of the observed time series would have been a better predictor than the model. The statistical index of model efficiency (Nash and Sutcliffe, 1970) is used,

$$Nash = \frac{\sum_{i=1}^{n}\left(O_i - S_i\right)^2}{\sum_{i=1}^{n}\left(O_i - \bar{O}\right)^2} \tag{8}$$

4. Bias. The optimal value of the Bias coefficient is (0), with low values indicate accurate model simulation. Positive values indicate underestimation and negative values indicate overestimation (Gupta et al., 1999) and can be represented by,

$$Bias = \frac{\sum_{i=1}^{n}\left(O_i - S_i\right)*100}{\sum_{i=1}^{n}\left(O_i\right)} \tag{9}$$

Furthermore, other visual plots to compare the observed and simulated rainfall amount by the ANN on seasonal basis are also considered.

3. Results& Discussions

Downscaling models are developed following the methodology described in Section 2. The results and discussion are presented in this section.

3.1 Potential Predictor Selection

The most relevant probable predictor variables necessary for developing the downscaling models for the four season's winter, spring, summer and autumn have been selected based on stepwise regression. The results in Table 1 show the selected predictors together with significance of the correlations for each season in terms of zero correlation and partial correlation (correlation of each predictor with the rainfall but take the effect of the other predictors). The most dominant predictor is the relative humidity at 850 hpa for the four seasons which reveals significance between 0.00-0.021 less than 0.05. The vorticity at 850 hpa and relative humidity at 500 hpa are ranked second for all seasons except the summer and spring. Other climate variables have been also considered as important (see Table 1) with a significance of 0.00-0.045, although the relative small correlation ranged between 0.038-0.351for zero correlation and 0.058-0.0256 for partial correlation.

In general 7 predictors were found to have a significant relation with the rainfall for winter, spring and 6 predictors for autumn while the summer shows only 4 predictors. Table 2 shows definition of each climate variable that has been used.

Table 1 selected Climate variable (predictors)

Predictors	JFD			MAM			JJA			SON		
	sig	Zero-order	Partial correlation	sig	Zero-order	Partial correlation	sig	Zero-order	Partial correlation	sig	Zero-order	Partial correlation
p_8z	.003	.143	.087	.000	.205	.139	-	-	-	.001	.067	.095
r850	.000	.252	.138	.000	.247	.256	.021	.045	.067	.000	.268	.250
P_v	.000	.325	.193	-	-	-	-	-	-	.000	.201	.212
P_f	-	-	-	-	-	-	-	-	-	.000	.132	.140
p_8f	.000	.351	.140	-	-	-	-	-	-	-	-	-
r500	.000	.332	.112	.000	.275	.122	.000	.154	.149	-	-	-
p_5th	.000	-.240	-.109	-	-	-	-	-	-	-	-	-
p_z	.003	.073	.086	-	-	-	-	-	-	-	-	-
p_5z	-	-	-	-	-	-	-	-	-	.002	.068	-.088
p_5u	-	-	-	.000	-.060	-.140	-	-	-	-	-	-
p_8v	-	-	-	.000	.237	.174	-	-	-	-	-	-
p_5f	-	-	-	.000	.065	.107	-	-	-	-	-	-
shum	-	-	-	.001	.096	.100	-	-	-	-	-	-
rhum	-	-	-	-	-	-	.000	.105	.123	-	-	-
p_8th	-	-	-	-	-	-	.045	.038	.058	-	-	-
p850	-	-	-	-	-	-	-	-	-	.000	-.126	-.131

*** sig**: significant level which is < 0.05 for significant correlation

Table 2 definition of the **s**elected climate variable

Code	Variable
r500	Relative humidity at 500 hpa
r850	Relative humidity at 850 hpa
P5_u	Zonal velocity at 500 hpa
p_z	surface vorticity
p5_z	500hpa vorticity
P8_z	850 hpa vorticity
rhum	Near surface relative humidity
p_8f	Surface airflow strength
P_f	Surface airflow strength
P_5f	500hpa airflow strength
p_v	Surface meridional velocity
p_8v	850 hpa meridional velocity
p850	850 Geopotential height
shum	Near surface specific humidity
P8_th	850 hpa wind direction

3.2 Model Performance

The selected climatic variables are provided as input to the regressions downscaling model together with the observed rainfall as output. For purpose of this study, 90% of the rainfall amount data considered as training set and 5% as validation set with additional 5% as test set after the training is stopped for the period 1961-2001 which were selected randomly. The validation set was used during the training to avoid the problem of overfitting. If the ANN is trained without stopping criteria (early stopping), then it begins to overfit, and the mean-square error begins increasing from its minimum. Without the early stopping method, data that have high complexity typically produce high variance when the training is terminated. The rainfall model has been applied using MATLAB 7.110.

Results of the different statistical properties of the observed and simulated rainfall model as defined in previous section are tabulated in Table 3 in terms of correlation coefficient (R), root mean squared error (RMSE), Nash coefficient and Bias. The results of statistical parameters analyses indicated good model simulation for rainfall because overly the relatively high R and Nash coefficient above 80% and 65% respectively for daily rainfall for all seasons. The RMSE and bias are considered relatively a bit high as it would not expect the model to replicate the exact daily sequences found in observations in an arid region.

Table 3 Statistical properties of ANN downscale model during calibration and validation periods

Coefficient	JFD	MAM	JJA	SON
R	0.84	0.81	0.84	0.85
RMSE	3.33	2.53	0.22	1.63
Nash	0.69	0.66	0.70	0.71
Bias	13.41%	-12.16%	-3.76%	-9%

Figure 4 shows comparisons of the observed and ANN estimated month-wise mean rainfall. Examination of Figure 4 shows that the calibrated model has reproduced the seasonal values quite well (during calibration and verification period). The model was slightly underestimated the mean monthly rainfall for January, February, March and December and overestimated May and September, while for the other months the model was in a good agreement. Hence the observed and the estimated annual rainfall are equal.

Further, examination of Figure 5 in terms of average monthly wet days, reveals that only for a few months (February, June, July and August), ANN simulated monthly mean almost equally low below that of the observed data. For all other months of the year, the model was over estimated the wet days.

It has been noticed that summer months were modelled better than the other season and that could be due to low skewness of the rainfall characteristics during this period.

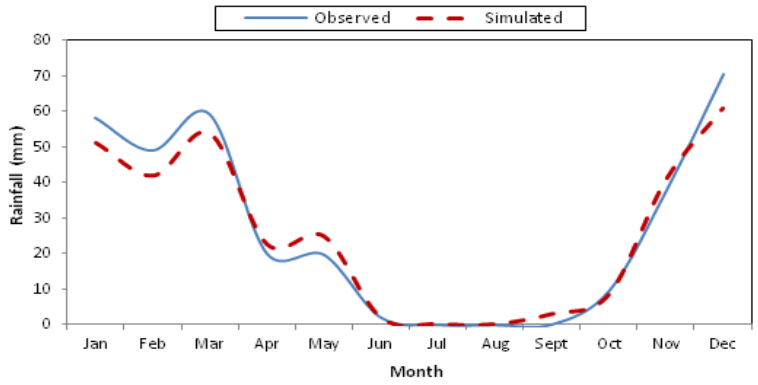

Figure 4 Average monthly rainfall of the observed & the simulated during calibration and validation periods (1961-2001)

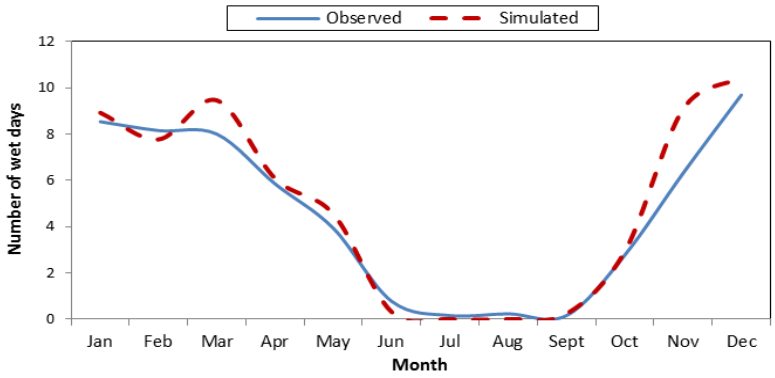

Figure 5 Average monthly wet days of the observed & the simulated during calibration and validation periods (1961-2001)

Another comparison for ability of ANN to reproduce the observed rainfall is quantile-quantile plot in Figure 6 between the observed and simulated daily rainfall for period 1961-2001. It is seen that the ANN model follow the 45° line for all daily rainfall amounts, suggesting the ANN models are closer to the observed rainfall distribution. There are outliers for the ANN model for high rainfall amount,

but not for low amounts in winter and spring seasons, which shows that low amounts are better simulated than high amounts, while the summer and autumn are more maintain the distribution.

Moreover, uncertainty in simulation of future extreme values using the ANN approach needs to be taken into consideration. For instance, if an event was not represented in the observed climate then it is unlikely to be represented in the future climate. So the ANN extremes performance produced from observed NCEP predictors was validated by comparing them with observed extremes. Extreme values, corresponding to specific return periods were estimated with a standard frequency analysis using Generalised Extremes Value Distribution (GEV, Coles (2001)) (see Figure 7). NN was able to reproduce the winter extremes properly while overestimate the daily extremes for the other seasons specially the autumn.

In general there are some differences between the observed daily rainfalls and simulated by ANN, but the overall performance of the downscaling model for calibration and evaluation phase at daily and monthly level is deemed satisfactory.

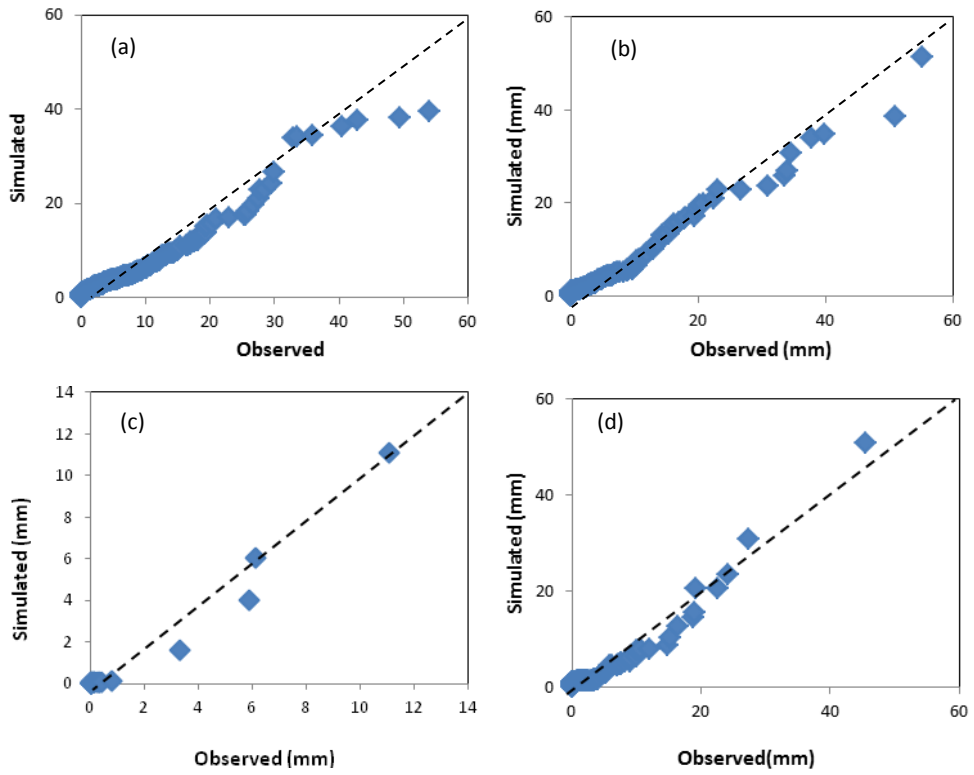

Figure 6 Quantile – Quantile plot for observed &simulated daily rainfall for (a) winter (b) spring, (c) summer and (d) autumn during calibration and validation periods (1961-2001)

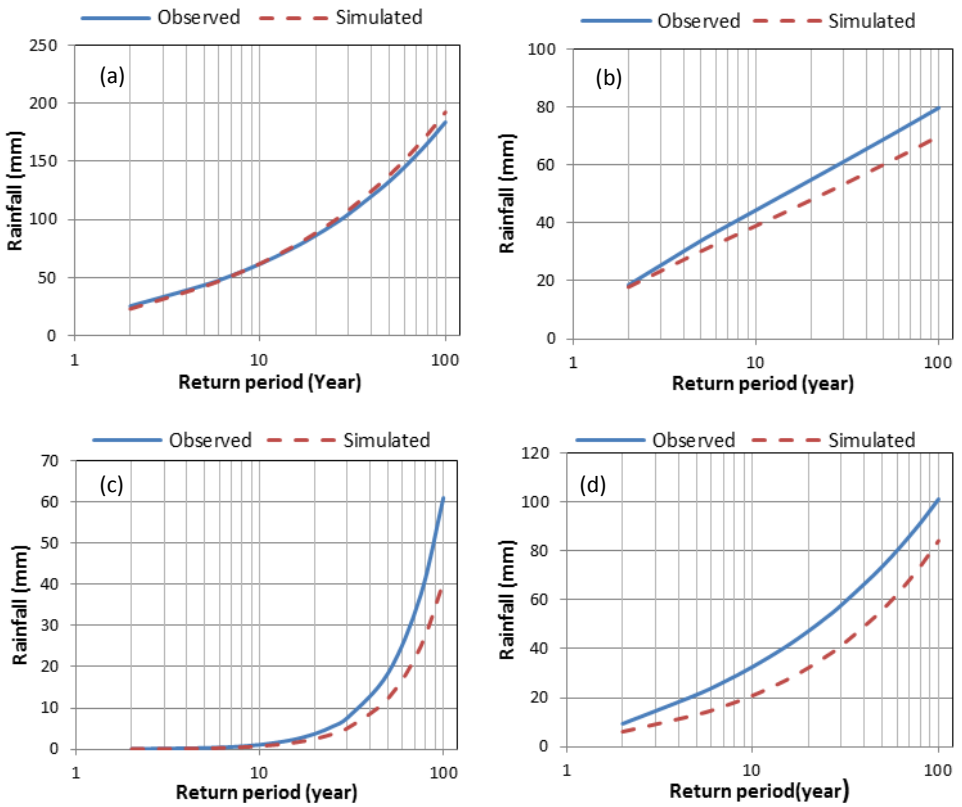

Figure 7 Return period-return level relationship of observed &simulated extremes rainfall for (a) winter (b) spring, (c) summer and (d) autumn during calibration and validation period (1961-2001)

The final Structures of the ANN used in building the models are shown in Figure 8. The suitable size and structure of ANN in terms of hidden neurones and weight were selected during the training process. It can be deduced from the network structures that the ANN modelling approach employs a larger number of neurons in the hidden layer in winter, spring & autumn and sometimes two hidden layers (12-20 neurons). This larger number of neurons in the hidden layer generally contributes to the accuracy of the model. In contrast, the summer model network uses smaller numbers of neurons in the hidden layer (one layer of 4 neurons).

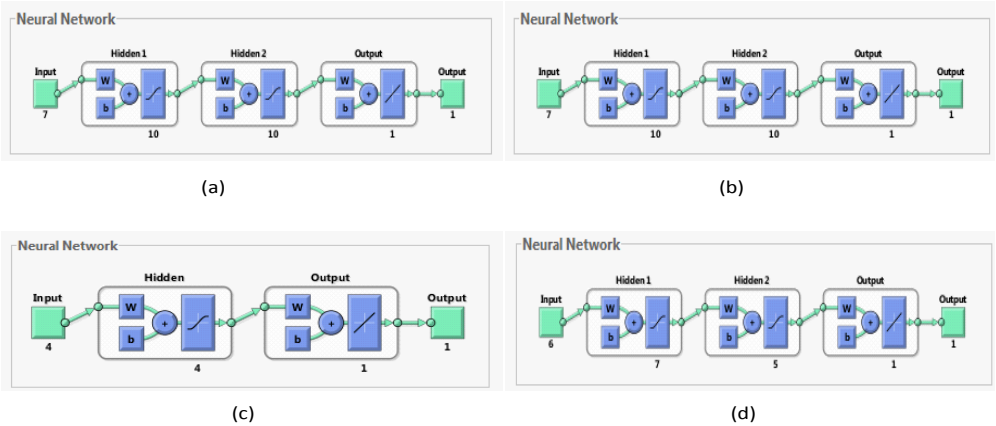

Figure 8 Structure of ANN models for (a) winter (b) spring, (c) summer and (d) autumn

3.3 Future Rainfall Projection

To incorporate the change in climate, one needs to calculate the relative change in daily mean wet and dry series lengths from the GCM output (HADCM3) of the control period (1961-1990) and future time-period.

From the bar chart of downscaled predictand (Figure 9), it can be observed that rainfall is projected to decrease in future for A2 and B2 scenarios. The patterns of rainfall in the future are relatively same for both scenarios although the B2 scenarios projected more reduction than A2 scenario. This is because among the scenarios considered, the scenario A2 has the highest concentration of atmospheric carbon dioxide (CO2). Generally a greatest reduction is anticipated in 2080s for most of the months and can be up to 96% and 58% as in June of A2 and March of B2 respectively. December experiences very a slight increase in 2020s for both scenario and same trend was obtained for January in 2050s.

Moreover, seasonal pattern of average daily rainfall for different future time slices for A2 and B2 simulations at Sinjar are also projected as shown in Figure 10. All seasons consistently projected a drop in daily rainfall for all future periods (black dots) with summer which expected to have more reduction compared with other seasons as it is consider to be almost dry by end of 21 century for both scenarios. A drop up to 34%, 45% and 30% for winter, spring and autumn respectively can be detected for A2 scenario by 2080s, while B2 projects a maximum drop of up to 34%, 30% and 33%. Vertical bar chart shows the standard deviation of the rainfall and confirmed that rainfall will be less variable and skewed due to the reduction of daily rainfall amount.

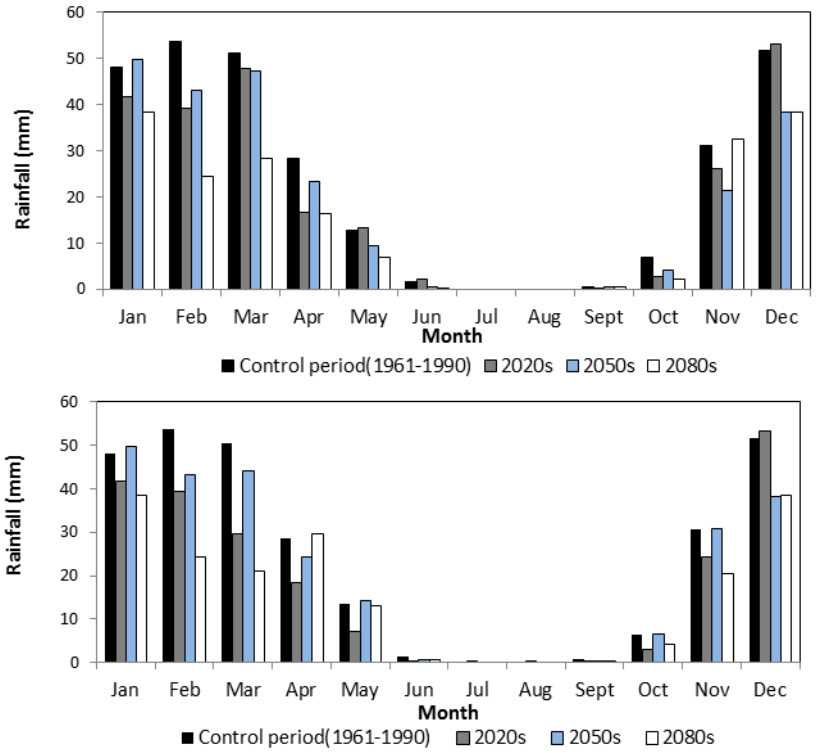

Figure 9 Future monthly average rainfall for different time slices for A2 scenario (upper) and B2 scenario (lower) compared with control period

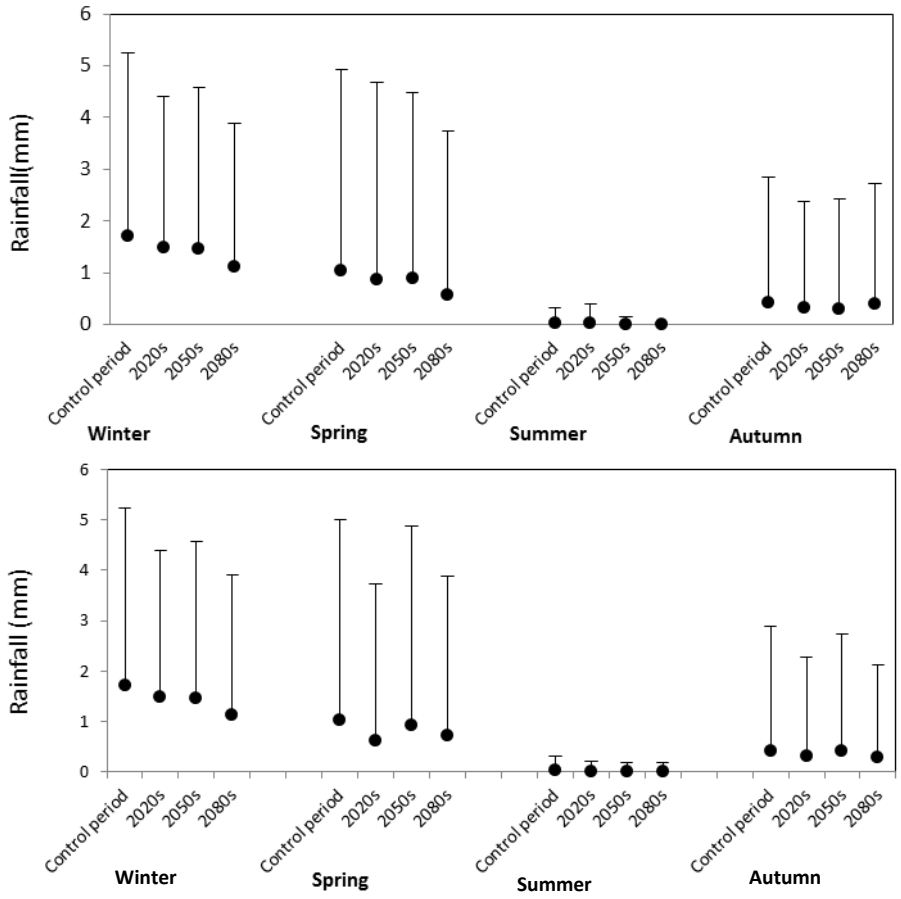

Fig 10 Seasonal average daily rainfall for different future time slices for A2 scenario (upper) and B2 scenario (lower) compared with control period. The vertical error bars indicate the standard deviation

Using a simple linear trend approach (Hannaford and Marsh, 2006), the gradient and its variance of the resulting regression of the hydrological series with respect to time is used to check the possible trends in the rainfall series for the period 1961-2099. Using Wald test, the significance of trend gradients is tested based on a normally distributed assumption. Figure 11 shows the series plots and their trend lines for the average annual rainfall for Sinjar station. The rainfall trend shows a significant downward for A2 and B2 scenarios ($\alpha < 0.05$) which confirm that climate change in Sinjar affect the rainfall pattern in a negative way especially in 2080s.

Figure 12 indicates that, there is an appreciable change in the number of wet days by 2080s for months January, February and March in both scenarios with about 10%-40% decrease in the wet days, while rest of the months experiences a slight drop for all future periods. No changes in summer months are noticed are they anticipated to be almost dry, however, a tendency of dryness extending to September is also observed (Figure 12).

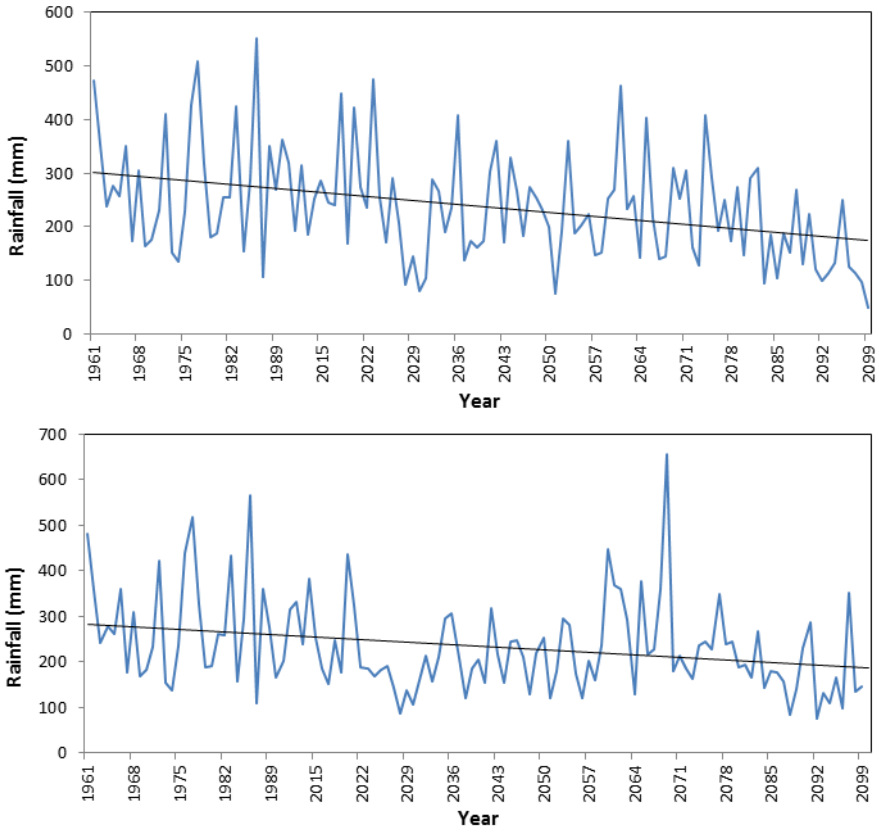

Fig 11 Average annual rainfall for A2 scenario (upper) and B2 scenario (lower) compared with control period. Linear trend indicates that there is a significant downward trend

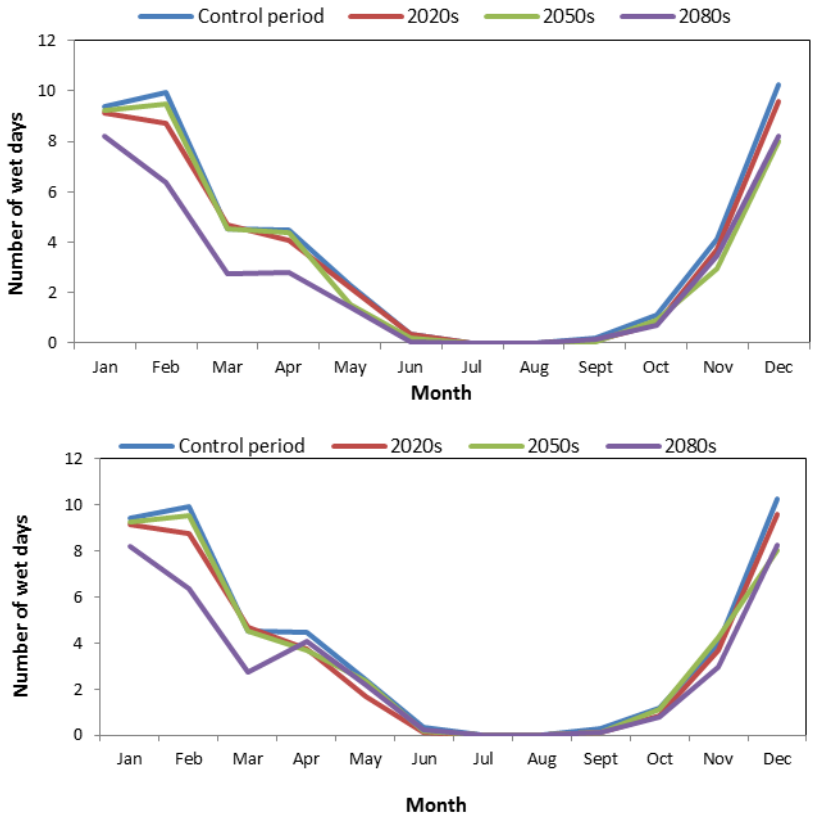

Fig 12 Average monthly wet days for A2 scenario (upper) and B2 scenario (lower) compared with control period

Figures 13, 14 shows a comparison of PDF estimates of GEV for current and projected daily annual extremes rainfall amount for Sinjar, which reveals a change in the shape of the distribution. The ANN model shows some increase in the extremes event of 2020s for A2 scenarios (the tail of distribution is shifted more to the right compared with the control period), while the other future period PDFs for same scenario relatively maintain the shape of distribution (Figure 13). The B2 scenario shows mix results for changes in the distribution of extremes event (Figure 14). The ANN model shows a decrease in higher amounts for the three future periods, while the model projects an increase in low rainfall amounts in 202s & 2050s, and decrease for in 2080s(the tail of distribution is shifted to the left) for the chosen GCM.

The ANN model is sensitive to the temporal changes in climatic variables, as it uses temporal features as well as point values in defining rainfall distribution. This may make the model very sensitive to small changes between scenarios, leading to different projections.

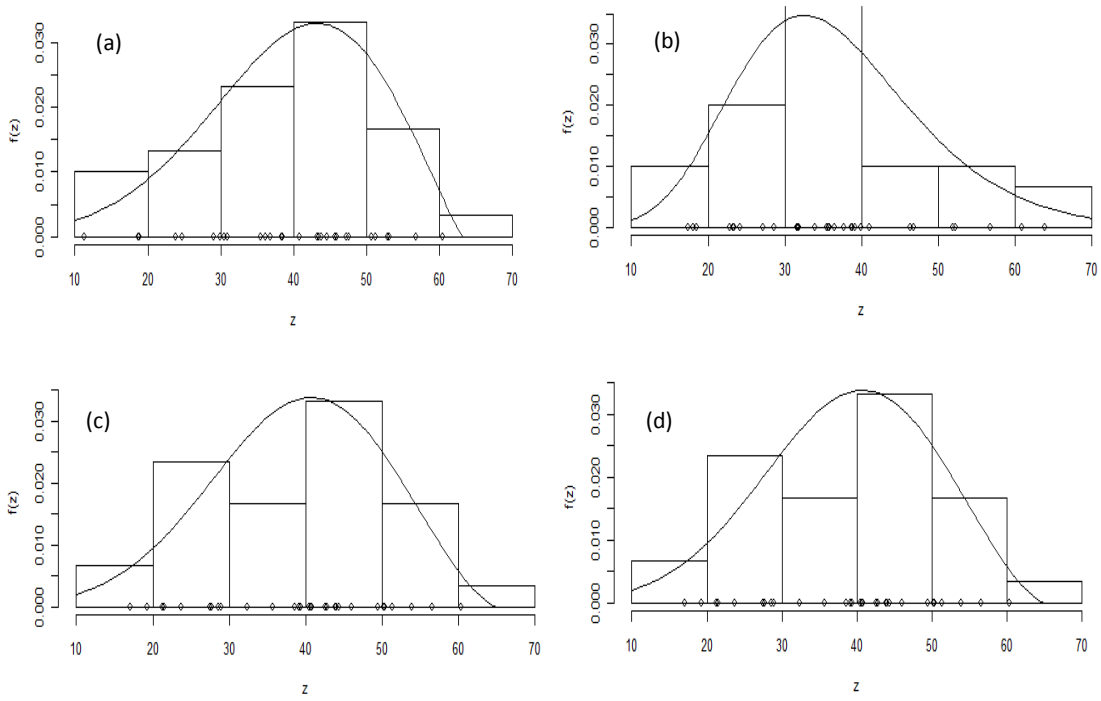

Fig 13 Probability density function distribution (pdf) of (a) control period compared with the future period for (b) 2020s (c) 2050s, (d) 2080s of annual extremes events for A2 scenario

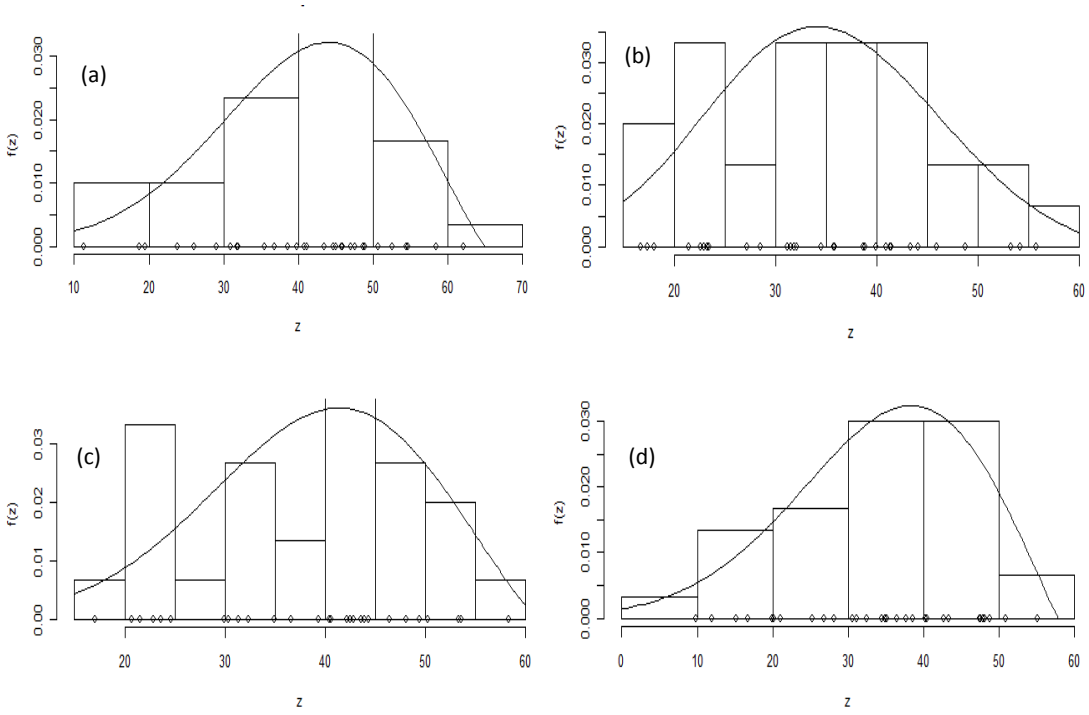

Fig 14 Probability density function distribution (pdf) of (a) control period compared with the future period for (b) 2020s (c) 2050s, (d) 2080s of annual extremes events for B2 scenario

In summary, it is evident that the average rainfall trend shows a continuous decrease. The overall average annual rainfall is slightly above 210 mm. This will keep this area below the average annual rainfall limit of 300mm required to maintain crop growth (FAO, 1987). Both scenarios (A2&B2) showed that about 83% of the years having rainfall less than 300mm. However, the distribution of dry years varies with time (Figure 15). In this figure there is a very slight increase of the average annual rainfall till 2060-70 followed by a sharp decrease towards 2099.

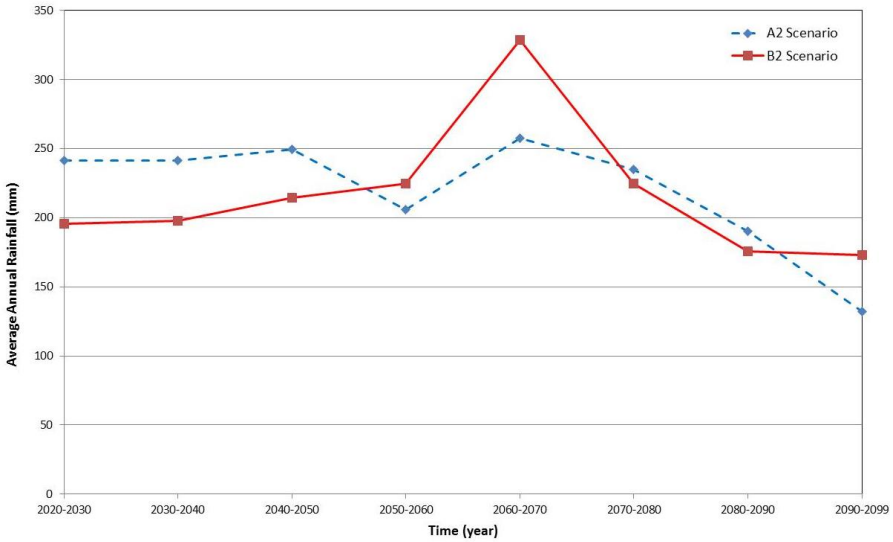

Fig. 15 : Change of average annual rainfall with time

4. Conclusions

Two emission scenarios used by the Intergovernmental Panel on Climate Change (A2 & B2) were used to study long term rainfall trends up to the year 2099 for Sinjar area northwest of Iraq. ANN model was used to provide climate change information to provide a suitable spatial scale from the GCM data. In general 7 predictors were found to have a significant relation with the rainfall for winter, spring and 6 predictors for autumn while the summer shows only 4 predictors. All seasons consistently projected a drop in daily rainfall for all future periods with summer which expected to have more reduction compared with other seasons as it is consider to be almost dry by end of 21 century for both scenarios.

The results also indicates that, there is an appreciable change in the number of wet days by 2080s for months January, February and March in both scenarios with about 10%-40% decrease wet days, while rest of the months experiences a slight drop for all future periods. No changes in summer months are noticed are they considered almost dry, however, a tendency of dryness extending to September is also observed. Generally the average rainfall trend shows a continuous decrease. The overall average annual rainfall is slightly above 210 mm. Both models showed that about 83% of the years having rainfall less than 300mm. However, the distribution of dry years varies with time. In this figure is slight increase of the average annual rainfall till 2060-70 followed by a sharp decrease towards 2099. In view of this prudent water management strategies are to be adopted to overcome water shortage crisis.

References

AL-Ansari, N.A. (2005). Applied surface Hydrology, Al al-Bayt University publication.

Al-Ansari, N.A. (1998) Water resources in the Arab countries: Problems and possible solutions. UNESCO International conf. (Water: a looming crisis), Paris, pp. 367-376.

Al-Ansari, N.A. (2013) Management of Water Resources in Iraq: Perspectives and Prognoses, J. Engineering, 5, 667-684.

Al-Ansari, N. A., Knutsson S. (2011) Toward Prudent Management of Water Resources in Iraq. Journal of Advanced Science and Engineering Research, 1, 53-67.

Al-Ansari,N.A. Al-Shamali,B. and Shatnawi, A., 2006, Statistical analysis at three major meteorological stations in Jordan, Al Manara Journal for scientific studies and research, 12, 93-120.

Al-Ansari,N.A., Baban, S. (2005)Rainfall Trends in the Badia Region of Jordan, Surveying and Land Information Science, 65(4), 233-243.

Al-Ansari, N.A.; Salameh, E. and Al-Omari, I., 1999, Analysis of Rainfall in the Badia Region, Jordan, Al al-Bayt University Research paper No.1, 66p.

Bazzaz, F. (1993). Global climatic changes and its consequences for water availability in the Arab World, in Roger, R. and Lydon, P. (Ed.), Water in the Arab Word: Perspectives and Prognoses, Harvard University, 243- 252.

Cavazos,T. Hewitson, B.C.(2005) Performance of NCEP variables in statistical downscaling of daily precipitation. Clim Res; 28, 95- 107.

Coulibaly, P., Dibike, Y.B. (2004) Downscaling Precipitation and Temperature with Temporal Neural Networks. J. Hydrometrology, 6(4), 483-496.

FAO, (1987) Improving Productivity of Dry land Areas. Committee on Agriculture (Ninth session). FAO, Rome. http://www.fao.org/docrep/meeting/011/ag415e/ag415e04.htm#4.1

Coles, S. (2001) An introduction to statistical modeling of extreme values, Springer,

Elasha, B. O. (2010) Mapping of Climate Change Threats and Human Development Impacts in the Arab Region, Uni- ted Nations Development programme, Arab Human Development Report (AHDR), Research Paper Series. http://www.arab-hdr.org/publications/other/ahdrps/paper02-en.pdf

Fistikoglu, O., Okkan, U. (2011) Statistical Downscaling of Monthly Precipitation Using NCEP/NCAR Reanalysis Data for Tahtali River Basin in Turkey. J. Hydrol. Eng., 16(2), 157–164. doi 10.1061/(ASCE)HE.1943-5584.0000300

Gupta, H.V, Sorooshian, S., Yapo, P.O. (1999) Status of automatic calibration for hydrologic models: Comparison with multilevel expert calibration. J Hydrologic Eng 4: 135-143.

Hewitson BC, Crane RG. Climate downscaling: techniques and application. (1996) Clim Res, 7, 85-95.

Hoai, N.D., Udo, K.., Mano, A. (2011) Downscaling Global Weather Forecast Outputs Using ANN for Flood Prediction. Journal of Applied Mathematics, Article ID246286, 14 pages doi:10.1155/2011/246286.

IPCC (Intergovernmental Panel on Climate Change), "Climate Change 2007: Climate Change Impacts, Adaptation and Vulnerability," Cambridge University Press, .

Jeong, D-I., Kim, Y-O. (2005) Rainfall-runoff models using artificial neural networks for ensemble stream flow prediction. Hydrol. Process 19(19), 3819–3835

Kalnay, E., Kanamitsu, M., Kistler, R., Collins, W., Deaven, D., Gandin, L., Iredell, M., Saha, S., White, G., Woollen, J., Zhu, Y., Leetmaa, A., Reynolds, B., Chelliah, M., Ebisuzaki, W., Higgins, W., Janowiak, J., Mo, K. C., Ropelewski, C., Wang, J., Jenne, R. & Joseph, D. (1996) The NCEP/NCAR 40-Year Reanalysis Project. Bulletin of the American Meteorological Society, 77 (3), 437-471.

Legates, D.R., McCabe, G.J (1999) Evaluating the use of goodness-of-fit measures in hydrologic and hydro-climatic model validation. Water Resources Research, 35 (1): 233-241.

Levenberg, K. (1944) A method for the solution of certain problems in least squares, Quarterly of Applied Mathematics, 5, 164–168.

Marquardt, D. (1963) An algorithm for least-squares estimation of nonlinear parameters, SIAM Journal on Applied Mathematics, 11(2), 431–441.

Naff, T. (1993) Conflict and water use in the Middle East, , in Roger, R. and Lydon, P. (Ed.), Water in the Arab Word: Perspectives and Prognoses, Harvard University, 253-284.

Lisboa, P.G.J. (1992) Neural Networks: current applications. Chapman & Hall, New York

Milly, P. C. D., Dunne, K. A and Vecchia, A. V. (2005) Global Patterns of Trends in Streamflow and Water Availability in a Changing Climate. Nature, 438, 347-350.

Nakicenovic, N., Davidson, O., Davis, G., Grübler, A., Kram, T., Lebre La Rovere, E., Metz, B., Morita, T., Peppe,r W., Pitcher, H., Sankovski, A., Shukl,a P., Swart, R., Watson, R., Dadi, Z. (2000)Emissions Scenarios. A Special Report of the Intergovernmental Panel on Climate Change. Cambridge University Press; Cambridge, UK.

Ojha, C.S.P., Goyal, M.K., Adeloye, A.J.(2010) Downscaling of Precipitation for Lake Catchment in Arid Region in India using Linea Multiple Regression and Neural Networks. The Open Hydrology Journal, 4,122-136.

Nash, J. E., Sutcliffe, J. V. (1970) River flow forecasting through conceptual models, Part I - A discussion of principles, J. Hydrol., 10, 282–290.

Rasheed, H., Mohammad, E., and Awchi, T. (1994) A field study on influence of initial moisture content on infiltration function. J. Al-Rafidain Engineering, 2 (3), 1-10.

Schaap, M.G., Leij, F.J. (1998) Database related accuracy and uncertainty of pedotransfer functions. Soil Science, 16, 765-779

Von,V., Heckl, A. (2011) Impact of Climate Change on the Water Availability in the Near East and the Upper Jordan River Catchment. Phd Thesis, University of Augsburg, Germany.

Trigo, R.M. (2000) Improving Metrological Downscaling Methods with Artificial Neural Network Models. PhD thesis, University of East Anglia.

UN, (2010)

Voss K., Famiglietti,J., Lo, M., de Linage, C., Rodell, M. and Swenson, S.(2013) Groundwater depletion in the Middle East from GRACE with implications for transboundary water management in the Tigris-Euphrates-Western Iran region, Water Resources Researc,49, 904-914.

Wheater, H. S. (2002) Progress in and prospects for fluvial flood modelling. Philosophical Transactions: Mathematical Physical and Engineering Sciences, 360 (1796), 1409- 431.

Yadav, D., Naresh, R., Sharma, V. (2010) Stream flow forecasting using Levenberg- Marquardt algorithm approach. IJWREE, 3(1), 30-40.